Chemical Papers (2023) 77:7319–7329
https://doi.org/10.1007/s11696-023-03007-8

ORIGINAL PAPER

Spectroscopic methods in the analysis of wear particles

Eva Švábenská[1] · Pavla Roupcová[1,2] · Oldřich Schneeweiss[1]

Received: 15 September 2022 / Accepted: 29 July 2023 / Published online: 23 August 2023

Abstract

Detailed characteristics wear particles formed in various brake pads were done. Our study was focused on identification structure and chemical composition of powder particles released by brake abrasion. The experimental studies were carried out using Mössbauer spectroscopy, X-ray powder diffraction, scanning electron microscopy and magnetic measurements. Structure and chemical composition of the original brake pads and disc samples were compared with the results obtained for wear particles. The chemical and phase composition of wear particles is in large part similar to composition of the original brake pads. Wear particles contained mainly various types of iron oxides, iron and iron carbon metallic particles. The part of the wear particles showed paramagnetic behaviour at room temperature. The sample with fully paramagnetic wear particles behaviour was subjected low temperature Mössbauer and magnetic measurements. The results indicate transition interval corresponding to magnetically ordered states—ferro/antiferromagnetic.

Graphic abstract

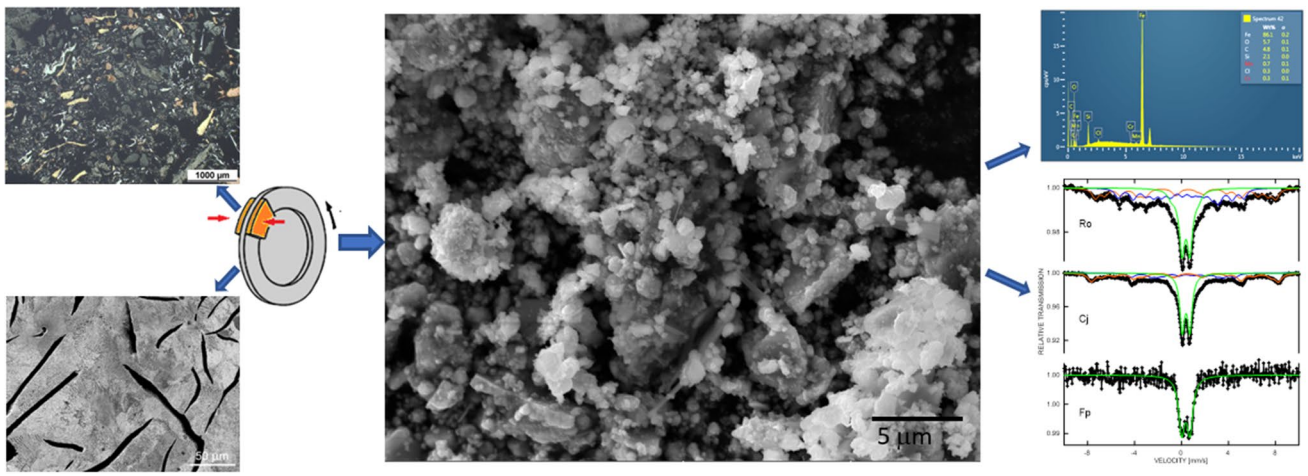

Keywords Mössbauer spectroscopy · Wear debris · Iron oxides · Fine particles · Brakes

Abbreviation

B_{hf}	Hyperfine induction (T)
IS	Isomer shift (mm/s)
Q_{Sh}	Quadrupole shift (mm/s)
Q_{Spl}	Quadrupole splitting (mm/s)
A	Atomic fraction of iron (a.f.)

✉ Eva Švábenská
svabenska@ipm.cz

[1] Institute of Physics of Materials, AS CR, v. v. i., Žižkova 513/22, 616 00 Brno, Czech Republic

[2] CEITEC Brno University of Technology, Purkyňova 656/123, 612 00 Brno, Czech Republic

Introduction

Exposure to airborne particulate matter (PM) can lead to a serious threat to human health (Maher et al. 2020; Kelly and Fussell 2020). Most particles breathed in the urban

atmosphere are extremely small (nanometric to a few micron size) and easily penetrate to airways. Metal-containing particles can be especially dangerous for humans, as they can enter all the major organs of the human body through the respiratory tract and bloodstream (Oudin et al. 2016). Air pollution increases the risk of multiple non-communicable diseases (Kelly and Fussell 2020). Exposure to particulate matter carries a higher risk of cardiovascular events (Maher et al. 2020; Hoek et al. 2013), neurodegenerative diseases (Maher et al. 2016) such as dementia (Peters et al. 2019; Oudin et al. 2016) or catalyze formation of damaging reactive oxygen species, leading to oxidative stress (Gerlofs-Nijland et al. 2019).

Parts of the PM have a natural origin. The source of these particles is wind erosion of soil, volcanic ash or sand from the desert. The humane activity is a source of further particles. Many particles are emitted by coal combustion, by industrial processes or in construction industry (Sanderson et al. 2014; Gonet and Maher 2019). In recent years has been growing proportion of particulate matter emitted by traffic. Potentially important components (about 50–85% depending on the location) of air pollutants are non-exhaust emissions consisting with brake wear, tyre wear, road dust and re-suspended PM (Ketzel et al. 2007; Boogaard et al. 2011). Size and chemical composition of particles emitted by non-exhaust sources may differ significantly and their percentage contributions to the atmospheric particles are quite site-specific. The non-exhaust emission affecting by some parameters, e.g. number of vehicles and mean speed, compositions of tyres and brakes of vehicles, type of roads, weather conditions (Valotto et al. 2015). It turns out that emissions from road vehicles are the primary source of metallic particles into the atmosphere (Boogaard et al. 2011; Oroumiyeh et al. 2022). Brake wear emissions play an important role, especially in the city (Bukowiecki et al. 2009; Lawrence et al. 2013). Urban dust also usually contains a significant amount of Fe-bearing particles (Valotto et al. 2015; Gunawardana et al. 2012) that might be especially in the form of fine and ultra-fine particles hazardous to neurological health (Gonet and Maher 2019).

One of the important sources of Fe-bearing particles are namely the components of the brake system (Sanders et al. 2003; Roubicek et al 2008; Hinrichs et al. 2011). The friction process carried out by the brake system is realized by means of (fixed) brake pads and a rotating brake disc. The brake disc is usually made of grey cast iron and its composition is relatively simple.

On the other hand, friction materials (brake pads), due to their composition, are amongst the most complex composite materials. Brake friction materials commonly consist of approximately 15–20 different components, which belong to one of four functional groups: additives, fillers, binders, and fibres (Chan and Stachowiak 2004; Adamiec 2017). Each of them has its own function and together they affect the frictional performance of a particular brake lining. Wear of counterparts (brake lining/pads and disc) contributes 60% of the total PM mass for this type (Sanders et al. 2003; Roubicek et al. 2008).

Mössbauer spectroscopy (MS) is extremely sensitive method for characterization of samples containing iron compounds. However, results of MS measurement for characterization of wear particles or samples of dust can be found sparse in articles. Probably the first application of MS for characterization of brake discs and pads was published team around Vasconcellos in 2010 (Vasconcellos et al. 2010). Pristine pads and discs together with worn friction couples, milled pristine pads, and some kind of raw materials used for pads manufacturing were tested in various geometries. Results comparing information from diverse analysis and depth as allowed by experiments performed in γ-transmission mode, backscattering geometry (BACK), counting conversion electrons (CEMS) or conversion X-rays (CXMS) emission.

During the friction test, when elevated pressures and temperatures are applied, changes in the phase composition may occur not only in the iron compound. Comparing the MS spectra of wear debris collected after brake dynamometer test and ball-milled sample showed that friction process has oxidizing character (Kukutschová et al. 2010). The composition of wear particles is also affected by vehicles speed before decelerating to full stops as shows experiments performed by Hinrichs et al. (2011). The Mössbauer spectrum from the milled pristine pad showed presence of raw materials commonly utilized in pad formulations—iron or some sort of steel as the major phase, magnetite and pyrite as a minor one. The high concentration of the magnetite was observed in the spectrum of particles related to the low speed (46 km/h). Compared to the spectrum from the high-speed debris (96 km/h) a major contribution represented iron and cementite, while magnetite was less important (Hinrichs et al. 2011).

The other studies take advantage Mössbauer spectroscopy for analysis iron-containing particles originate from industrial dust (Magiera et al. 2011), road dust (Szumiata et al. 2013; Górka-Kostrubiec et al. 2019; Muxworthy et al. 2002; Wang 2016) or aerosol fraction (Kopcewicz et al. 2015). Sometimes road dust analyses were accompanied by measurements of magnetic properties in addition to MS analyses (Górka-Kostrubiec et al. 2019). The results show that different type of metallic iron contained in road dust is mainly an anthropogenic origin. Mössbauer spectra obtained for dust from different sources confirmed dominant contribution of magnetite, with the significant presence of α-Fe-phase in ferromagnetic state and hematite. The contribution of paramagnetic components was very significant (Górka-Kostrubiec et al. 2019). The presence of metallic α-Fe particles on

micrometre size (Górka-Kostrubiec et al. 2019) was also recognized in similar studies (Muxworthy et al. 2002; Szumiata et al. 2013).

The primary aim of the research study was used the combination of spectroscopic methods with scanning electron microscopy and X-ray powder diffraction for evaluations of chemical and phase composition and morphology of wear particles from automotive brake systems. The main focus was on iron, its compounds and iron-containing particles. Analyses and their interpretation will provide a more complete picture of the types of iron-containing brake wear particles and their potential sources.

Experimental

Materials

The brake pads were obtained from a service repairing passenger and light commercial vehicles. The wear particles were collected by sweeping of brake pads. Prior to analysis, the brake pad samples from different cars and the brake disc (only one car) were cut into smaller samples by a diamond disc saw. The samples of brake pads now had dimension approximately 30 × 30 × 8 mm and comprised representative part of each samples. Afterwards, the samples were grinding and polishing in a metallographic laboratory before further analysis and microscopic observation. The brake pads samples were marked with abbreviation Cj, Ro, and Fp.

Analytical methods

The brake pads and disc, as well as the collected wear debris were analysed using combinations of several analytical techniques: Mössbauer spectroscopy, Glow discharge optical emission spectrometry (GDOES), X-ray fluorescence (XRF), X-ray powder diffraction (XRD), scanning electron microscopy (SEM) and magnetic measurement.

Chemical composition of brake pads was obtained in Olympus Vanta analyser highly advanced handheld XRF device. Analysis were performed via GEOCHEM mode, which is a calibration done by the manufacturer. Chemical analysis of brake disc was done by GDOES using GD-Profiler 2 instrument with the Quantum™ XP software operating in radio frequency at 15.56 MHz. Analysis were performed via calibrated method (Fe-bulk) with usage 4 mm of internal diameter copper anode and optical spectrometer on 0.5 m Paschen Rounge polychromator. The wavelengths of the spectral lines were as follows 372 nm for Fe, 165 nm for C, 288 nm for Si, 403 nm for Mn, 425 nm for Cr, 324 nm for Cu, 180 nm for S, and 178 nm for P.

The surfaces of the brake pad samples and wear particles were investigated by SEM Tescan LYRA 3 XMU FEG/SEMxFIB equipped with X-Max80 EDS detector for X-ray microanalysis by Oxford Instruments with the Aztec control system. The prepared samples were observed at an accelerating voltage of 10 kV. The accelerating voltage used for EDS mapping and chemical analysis was increased to 15 kV.

The phase studies were carried out with Empyrean automatic diffractometer (PanAnalytical) using CoKα radiation with qualitative analysis by HighScore® software and the ICDD (PanAnalytical database.

^{57}Fe Mössbauer spectroscopy was carried out in transmission geometry with detection of 14.4 keV gamma radiation (MS) using a standard Mössbauer spectrometer in a constant acceleration mode with a ^{57}Co (Rh) radioactive source. The spectra were measured in temperature range 5–293 K. A pure α-Fe foil was used as a calibration standard for the velocity scale. The computer processing of the spectra was done using CONFIT program package (Žák and Jirásková 2006). The samples (about 70 mg powder) were closed in Al foil capsules 10 mm in diameter which ensure the thermal contact of the measured powder in the cryostat.

Magnetic measurements were carried out using Physical Property Measurement System EverCool II (2–400 K, 0–9 T) with vibrating sample magnetometer. The temperature dependence of magnetic moment was measured in temperature range 2–380 K in 100 Oe magnetic field after zero field cooling and field cooling by decreasing temperature.

Results

Characterization of brake lining

The individual brake lining samples had significant differences between them as shown the results for chemical and phase analysis (Supplement Table S1 and S2). The elemental composition of brake pads was diverse. According to XRF analysis, about around 50 wt.% of compositions were consisted by light elements (LE) like C, N, and O. The sample Cj contained 56 wt.%, sample Fp 51 wt.%, and the last sample Ro contained only 40 wt.%. The comparison XRF and SEM/EDS results shown that samples contained around 45 wt.% of carbon. Carbon is present mostly in the form of graphite, carbon fibres, or as a phenol–formaldehyde resin binder. In addition to well-crystalline graphite, the carbon present in the XRD results as broad peaks well hidden in the background interpreted as amorphous or nanocrystalline material.

The significant iron content was observed in all samples. Sample Ro and Cj contained around 13 wt.%, while sample Fp contains around 8 wt.% of iron. The iron was present in the form of iron chips (Ro and Fp) or various iron oxides (Cj and Ro) according results from XRD analysis and SEM observation. The different types of brake pads have been

comprised from various friction components. Magnetite (Fe_3O_4) present in samples (Ro and Cj) can act as both an additive and a modifier.

The constitution of the Ro and Cj samples is relatively similar in terms of chemical composition. In the comparison of Cj and Ro samples with Fp sample, these have common only presence of amorphous phase, carbon and iron. Chemical elements discovered in a larger quantity in at least one sample were Cu, Mg, Ca, Ba, Si, Zn, Sb, S.

The source of copper observed in the sample Ro was formed by brass chips (Cu and Zn alloy) but also pure copper chips as showed XRD analysis. On the other hand, copper presented in the sample Cj was in the form metal sulphides as chalcopyrite $CuFeS_2$. Sulphur was also bound in the minerals stibnite (Sb_2S_3) and barite ($BaSO_4$), both observed in samples Ro and Cj. Abrasives as an aluminium silicon oxide ($Al_{4,544}\ O_{9,728}\ Si_{1,456}$) and silicon dioxide ($SiO_2$) were detected in the sample Cj. In the Fp sample were observed 28 wt.% calcium carbonate ($CaCO_3$) performing functions of inorganic fillers and around 18 wt.% of magnesium oxide (MgO) in the function of modifiers.

Characterization of brake disc

The analysed brake disc came from the same car as the sample of brake pads Cj. Similar as in previous study (Švábenská et al. 2015a, b), brake disc was manufactured from grey cast iron. The chemical composition was determined by GDOES and microstructure of the sample was observed by SEM. The grey cast iron of brake disc was composed from 2.8 wt.% of carbon, 1.9 wt.% of silicon, 1 wt.% manganese, with negligible amount of trace elements (chromium, copper, sulphur and phosphorus).

Carbon was present in the form of graphite "flakes" in a pearlitic matrix. Figure 1D shows pearlitic matrices structure with graphite flakes etched by 2% Nital and small amount of inclusions. The inclusions were formed by MnS, FeS and SiO_2.

Characterization of wear particles

Shape and types of particles

The next step was study of wear particles originate from interaction of brake pads samples and brake disc. Irregular shapes of wear particles shows images obtained by SEM (Fig. 2). The size distribution of the particles was very wide. The biggest particles achieved size with around 200–500 µm, through middle particles with approximately 30 µm size to the small particles with 1 µm diameter roughly and less. Small particles were found on a large scale in all samples.

Particles in ranges of nm were observed mainly in the form of agglomerates or as a globular feature captured on the surface of larger particles. In the case of Cj and Fp samples, long fibres contained especially carbon were noted.

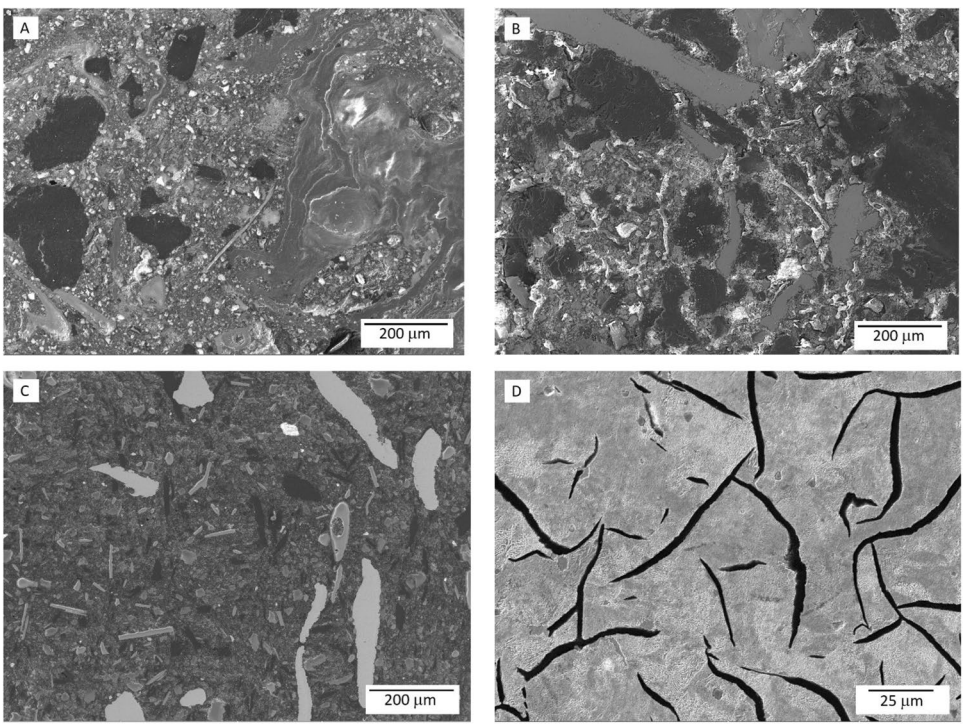

Fig. 1 SEM images of brake lining samples Cj (**A**), Ro (**B**), Fp (**C**) and microstructure of brake disc made from grey cast iron (**D**)

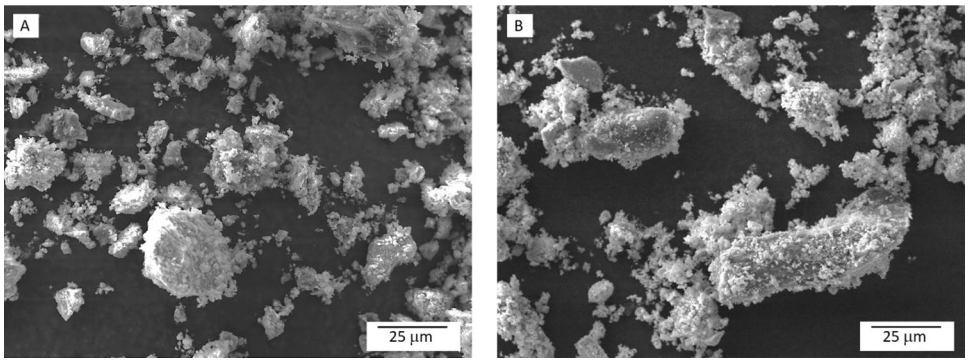

Fig. 2 SEM images of brake wear particles obtained from sample Cj (**A**) and Ro (**B**)

Table 1 The phases (weight percent) presented in wear particles according XRD measurements

Phase	Formula	Sample		
		Ro	Cj	Fp
Carbon/graphite	C	1	1	
Iron/ferrite	α-Fe			11
Hematite	Fe_2O_3	46		52
Goethite	FeO·(OH)		33	22
Magnesium diiron (III) diodixe	$(MgFe_2)O_4$	42	35	
Iron (II) Iron (III) aluminium hydroxide sulphate hydrite	$(Fe_2(Fe_{0.76}Al_{0.24}))\cdot(OH)_6(SO_4)_{0.5}(H_2O)_{2.4}$	2		
Chalcopyrite	$CuFeS_2$			1
Zhanghengite	CuZn			1
Manganese iron carbide	$(Mn_4Fe_3)C_3$	8		
Calcite	$CaCO_3$	1		
Coesite	SiO_2		6	
Quartz low	SiO_2		20	13
Barite	$BaSO_4$		5	

Phase and chemical composition

The wear particles predominantly contain iron according to EDS analysis. XRD results also confirmed that the wear particles contain 80 or more weight percentage of iron-containing compounds. These iron compounds have been constituted by various iron oxides, iron hydroxides and Fe (0). The phase composition of wear particles samples is present in Table 1.

Except predominant iron, samples of wear particles contained small amount of the further elements that correspond with original composition of brake pads. The compounds incorporate these elements (Si, Ba, Ca, Cu, Ba, Al, Mg, Mn, etc.) contained either small dispersed particles and/or were observed trapped on other, larger, predominantly Fe-bearing particles (Fig. 3). The phase analysis of abrasion particles provides other information about the distribution of elements

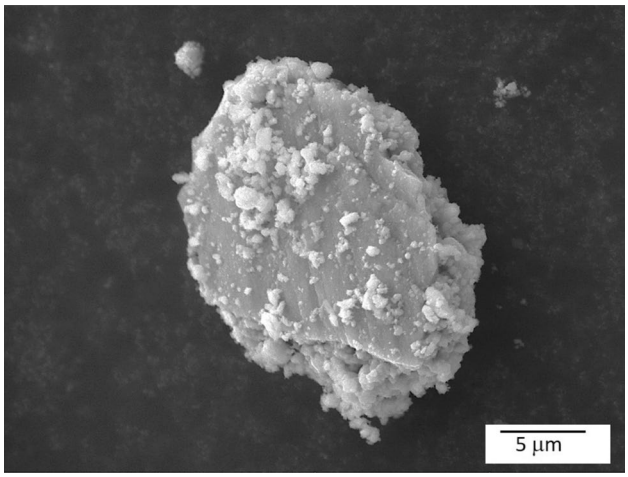

Fig. 3 Detail of wear particle with trapped smaller particles

(Table 1) as well as elements mapping by SEM/EDS (Fig. S1 in Supplementary data).

Mössbauer spectroscopy

Mössbauer spectroscopy was used for more detailed identification of wear particles containing Fe. The spectra were measured in the temperature range 5–293 K. Spectra analysis yields the relative contents of individual Fe-containing phases in atomic fraction of iron (A) and corresponding hyperfine parameters of phases: isomer shift (IS), quadrupole shift (Q_{Sh}) and quadrupole splitting (Q_{Spl}), and hyperfine induction (B_{hf}) (Gonser 1975).

Measured Mössbauer spectra are shown in Fig. 4. The main component of the spectra of all samples is the doublet representing paramagnetic phases. In the spectra of Ro and Cj samples minor sextets can be observed. The fitted components were divided into three groups and ascribed to the following phases: (1) Fe based oxides particles with magnetic splitting, (2) metallic particles of iron and iron carbon—$Fe + Fe_3C$, and (3) paramagnetic particles. Their

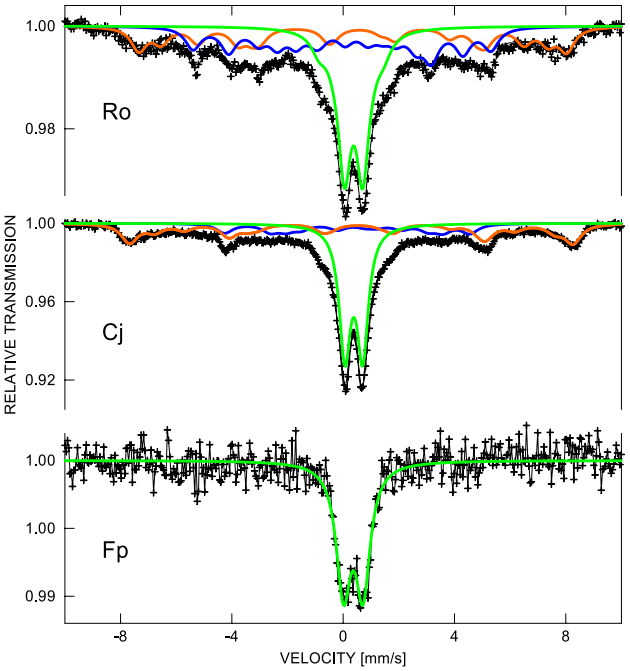

Fig. 4 Mössbauer spectra with fitted components: Fe based oxides (orange line), Fe + Fe_3C (blue line), and paramagnetic particles (green line)

Table 2 Contents of phase groups in atomic fraction of iron atoms for samples measured at 293 K

Sample	Fe based oxides	Fe + Fe_3C	Paramagnetic particles
Ro	0.29	0.34	0.37
Cj	0.30	0.20	0.50
Fp	–	–	1.00

contents (in atomic fraction of iron atom) are reported in Table 2.

The hyperfine parameters resulting from the Mössbauer spectra analysis of individual samples are present in the Tables 3, 4, and 5.

The content of paramagnetic phases in Ro sample reaches 0.36 atomic fraction of iron. They are represented by doublet with IS ≈ 0.37 mm/s and Q_{Spl} ≈ 0.68 mm/s. The spectrum contained also several sextets with parameters corresponding to various Fe^{3+} oxides and sextets which can be ascribed to an iron carbide and alpha iron phases.

The similar situation is also in the case of sample Cj. The doublet is more dominant than in the sample Ro and splitting to sextets is not such noticeable. The amount of paramagnetic particles is an increasing and the component including Fe + Fe_3C fraction decreasing.

In the spectrum of Fp sample mainly the component of paramagnetic particles (doublets) was found. The occurrence of paramagnetic fraction can be ascribed to presence of fine nanocrystalline particles (≤ 10 nm). This consideration corresponds with XRD results, when the size of nanocrystals (according to their coherent length) of hematite (≈ 52 wt.%) and iron (II) oxide hydroxide (≈ 22 wt.%) was about 8 nm for main fraction of the sample. Another phase, appointed as iron was the crystalline size approx. 30 nm.

Another series of experiments was performed to obtain more detailed information about the paramagnetic particles in the Fp sample. The blocking temperature of the dominant part of the particles was determine by measurements in the selected temperature range. Based on these data, the temperatures for the MS spectra measurements were chosen.

The temperature dependence of magnetic moment as zero field measurement (ZFC) and field cooled in 100 Oe external field (FC) was measured in temperature range 5–295 K. The results for Fp sample are shown in Fig. 5. The maximum on the ZFC curve corresponds to the blocking temperature of the dominant part of the particles. The subsequent decrease has two reasons. The first one is temperature dependence of

Table 3 Hyperfine parameters resulting from the Mössbauer spectra analysis of sample Ro

Component	IS (mm/s)	Q_{Sh} (mm/s)	Q_{Spl} (mm/s)	B_{hf} (T)	A
S1	0.419 ± 0.018	− 0.23 ± 0.03		48.0 ± 0.1	0.11 ± 0.01
S2	0.417 ± 0.017	− 0.25 ± 0.04		43.9 ± 0.2	0.08 ± 0.01
S3	0.311 ± 0.016	0.02 ± 0.04		38.0 ± 0.2	0.08 ± 0.01
S4	0.004 ± 0.003	− 0.01 ± 0.02		32.8 ± 0.1	0.15 ± 0.01
S5	0.346 ± 0.017	− 0.65 ± 0.04		26.1 ± 0.1	0.11 ± 0.01
S6	− 0.065 ± 0.020	− 0.05 ± 0.04		15.0 ± 0.1	0.11 ± 0.01
D1	0.371 ± 0.005		0.68 ± 0.01		0.32 ± 0.01
D2	0.424 ± 0.014		2.52 ± 0.04		0.04 ± 0.01

IS—isomer shift, Q_{Sh}—quadrupole shift, Q_{Spl}—quadrupole splitting, B_{hf}—hyperfine induction, A—phase content in atomic fraction of Fe

Table 4 Hyperfine parameters resulting from the Mössbauer spectra analysis of sample Cj

Component	IS (mm/s)	Q_{Sh} (mm/s)	Q_{Spl} (mm/s)	B_{hf} (T)	A
S1	0.404 ± 0.013	− 0.25 ± 0.03		49.57 ± 0.1	0.17 ± 0.01
S2	0.612 ± 0.024	− 0.44 ± 0.05		44.93 ± 0.2	0.08 ± 0.01
S3	0.209 ± 0.023	− 0.07 ± 0.04		36.81 ± 0.2	0.06 ± 0.01
S4	0.004 ± 0.003	− 0.90 ± 0.07		28.31 ± 0.3	0.05 ± 0.01
S5	0.515 ± 0.026	− 0.54 ± 0.05		28.09 ± 0.2	0.08 ± 0.01
S6	0.040 ± 0.031	− 0.24 ± 0.05		16.22 ± 0.2	0.08 ± 0.01
D1	0.361 ± 0.004		0.65 ± 0.01		0.44 ± 0.01
D2	0.221 ± 0.017		1.93 ± 0.04		0.04 ± 0.01

Table 5 Hyperfine parameters resulting from the Mössbauer spectra analysis of sample Fp

Component	IS (mm/s)	Q_{Sh} (mm/s)	Q_{Spl} (mm/s)	B_{hf} (T)	A
S1	0.028 ± 0.019	− 0.08 ± 0.03		32.64 ± 0.1	0.12 ± 0.01
S2	0.196 ± 0.053	− 0.45 ± 0.10		25.97 ± 0.3	0.04 ± 0.01
D1	0.376 ± 0.001		0.72 ± 0.01		0.84 ± 0.01

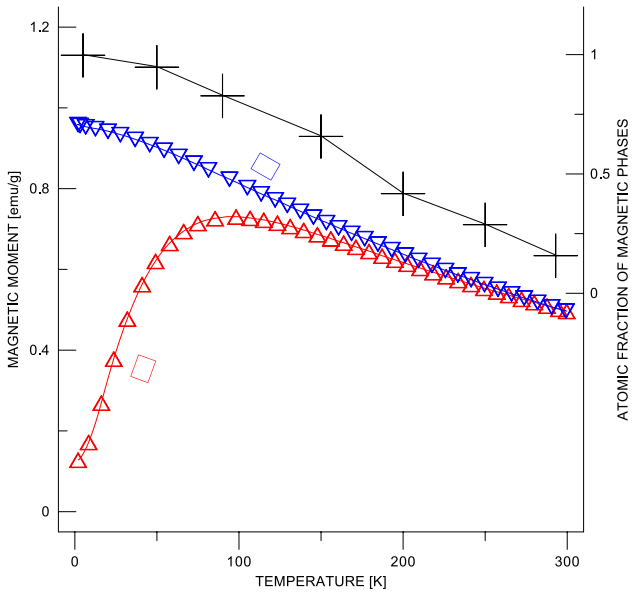

Fig. 5 Temperature dependences of magnetic moment (ZFC △, FC ▽) and atomic fraction of magnetic components in Mössbauer spectra (+)

the magnetic moment and the second one is transition of the part of particles to the paramagnetic state.

The examples of the Mössbauer spectra taken in the temperature range 5–293 K are drawn in Fig. 6. The content the doublet (red line in the figure) in the spectra can be ascribed to the atomic fraction of the paramagnetic phase. Its decrease with increasing temperature corresponds with the FC curve. This result is drawn in Fig. 5.

The appearance of the MS spectra changes around 90 K, which is the blocking temperature for this sample. The doublet of the paramagnetic phase is suppressed at lower temperatures and splitting corresponding mainly to hydroxide particles is present.

The low temperature measurement at 5 K (Fig. 7) indicates that the main components with mean hyperfine inductions B_{hf} in the range 52.6–43.6 T and isomer shifts IS from 0.51 to 0.41 mm/s with sum of atomic fractions A of 0.88 represent the various iron oxides particles. The remaining components can be ascribed to an iron carbide ($A \approx 0.03$) the metallic debrises ($A \approx 0.06$) from the brake disc and paramagnetic phases reach 0.02 atomic fraction of iron. Detail information about hyperfine parameters resulting from the Mössbauer spectra measurement are available in Supplement Table S3.

Discussion

The realized analyses provided data on the composition of the brake pads and disc, when special focus was placed on iron compounds. In his comprehensive study of the elemental composition of automotive brake materials, Hulskotte reported an iron content ranging from 20 to 85% (Hulskotte et al. 2014). These values are much higher than our observed range of 8–13%. The contrast between the results is due to the exclusion of certain elements (C, O, and Mg) from the total in Hulskotte's study.

In the case of our brake pads iron chips, iron oxides (magnetite, wűstite) or as a mixed sulphide (chalcopyrite) are compounds containing iron according to XRD. The size spectrum of components making up brake pads is very wide, ranging from hundreds of micrometres to hundreds or tens of nanometers. Fe containing components shows similar trend in size. Iron chips, which improve toughness and strength, are approximately 300 µm long and a 50 µm wide;

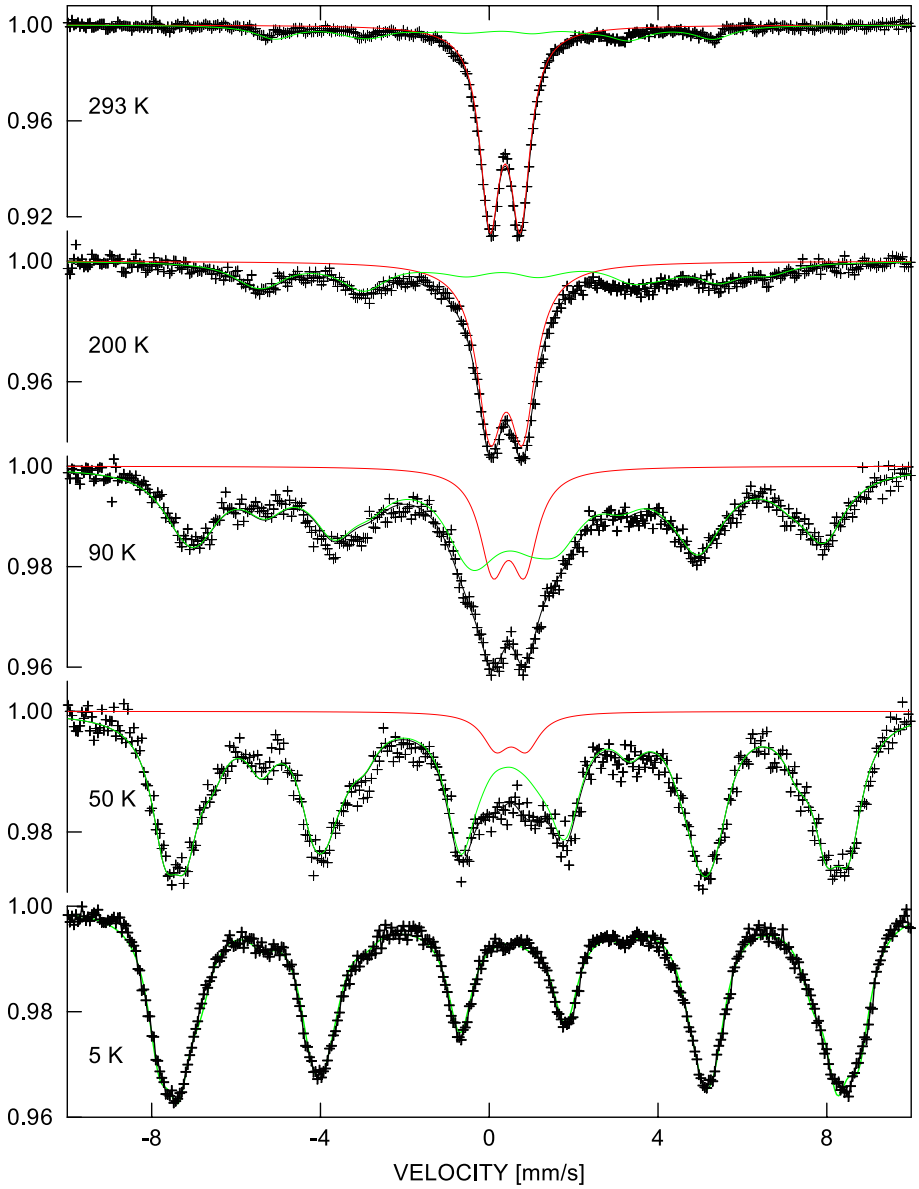

Fig. 6 Examples of Mössbauer spectra taken at indicated temperatures. The red line represents fitted component of paramagnetic phases and the green line the magnetic (ferro- or antiferromagnetic) phases

iron oxides and sulphides, which act as lubricants and mild abrasives, are around 50 µm and smaller in size. The iron content in the brake pads and in the wear particles released from them differ not only in size, but also in the iron content. The size of the observed wear particles descent from the largest with a size around 500 µm to nanometer-sized particles. It was also found that the percentage of iron particles in the samples of wear particles reached approx. 70–90%.

A dominant sextet indicating the presence of Fe^{3+} and/or Fe^{2+} oxides was expected based on published MS analyses of brake pads and debris collected after brake dynamometer test (Kukutschová et al. 2010; Vasconcellos et al. 2010). However, our results show that the main component of the spectra of all samples is the doublet representing paramagnetic phases. The paramagnetic doublet was observed in study by Hinrichs et al. (2011), where the effect of friction coefficient tests on the phase characterization of wear particles generated from brake pads was studied. According to the results, the composition of the debris appears to be related to stopping from different speeds. The spectrum of particles originating from test at a lower speed (48 km/h) had a very intense central doublet of paramagnetic pyrite compared to the spectrum of particles from tests at higher speed (96 km/h) (Hinrichs et al. 2011). Pyrite is a fairly common component of brake pads, but in our case, according to XRD analysis, it was not represented in the samples. The pyrite MS parameters are similar to the doublet-like features parameters of the superparamagnetic small sizes particle at room temperature. The low temperature MS measurements showed presence of various iron oxides.

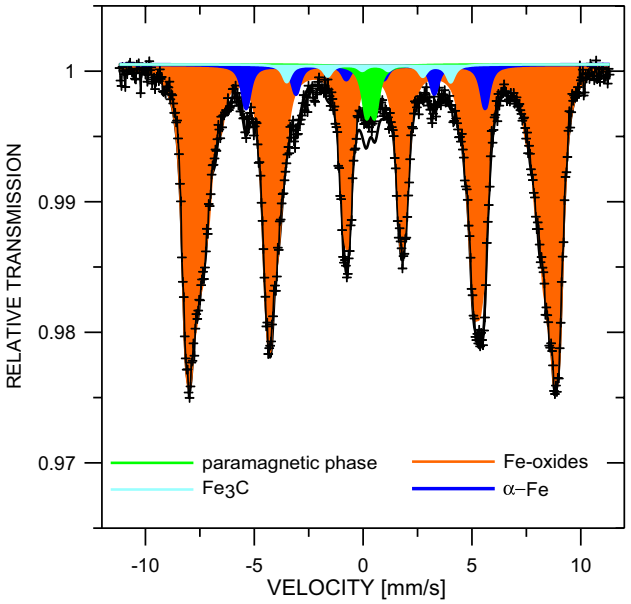

Fig. 7 Mössbauer spectrum of the Fp sample measured at 5 K

Unfortunately, the results amongst studies are comparable only to a limited extent. One of the reasons why it is difficult to compare the results is the way the wear particles are obtained. Wear particles prepared by milled showed dissimilar representation of especially iron phases to particles from dynamometer test or obtained by sweeping (Kukutschová et al. 2010; Vasconcellos et al. 2010; Hinrichs et al. 2011; Švábenská et al. 2015a, b, Nanocon). It is possible to expected that the similar trend will be also in wear particles prepared by dynamometer test and obtained in real driving condition where the influence of the environment and weather conditions can also be assumed.

The other factor is composition of original brake pads. As was mentioned earlier, the brake pads composition is very changeable (producer, type of car, driving style, etc.) and number of input components are very extensive. The individual studied samples differed in the content of the input components and their representation. In addition, the composition of brake-wear particles significantly differs from of the original lining material. This is due to the wide variability of resistance to mechanical disintegration and also degradation and volatilization across various chemical components.

A detailed examination of wear particles Fe-bearing by MS in our case therefore demonstrated the occurrence of particles in the form various Fe^{3+} oxides, iron carbide, alpha iron phases and amount of paramagnetic particles. Wear particles were produced during braking by worn out from the pad and disc. It looks like the contribution of the disc will be more significant than that of the brake pads. This is evidenced by the presence of iron carbide and alpha iron, the source of which will be the brake disc.

The coarse and fine wear Fe particles come into existence by a mechanism probably involving the action of the hard constituents of pads like as abrasives. However, sand, particle of soil, deicing chemicals and other impurities occurring in road environment can also work like an abrasive. When compare two systems of brake—drum and disc; lining together with brake disc produce more wear particles than lining mounted in closed brake drums. On the other hand, brake discs provide very effective way of braking in comparison with brake drums and make cars operation safer.

The paramagnetic behaviour of part the samples can be ascribed to presence of fine nanocrystalline particles (≤ 10 nm). This assumption is confirmed by the XRD results as well as our unpublished transmission electron microscope observations.

Conclusions

The present work aimed at elucidating the morphology and chemical composition of the brake system components, together with analysis of the brake wear particles. Samples has been studied using a combination of Mössbauer spectroscopy, powder X-ray diffraction and microscopy. The study indicated that the composition of the original material of the brake pads is also reflected in the composition of the released wear particles.

- The iron oxides and hydroxides originated mostly from brake wear from the frictional layer that forms between cast iron disc and pads or linings.
- Metallic Fe(0) and iron carbide have originated from brake disc.
- In all samples, a certain fraction showed paramagnetic properties. In this case, this property was related to the size of the particles, which according to the analyses were the fine nanocrystalline particles (≤ 10 nm).

Although the presented results confirmed former observations the size and chemistry of wear debris represents a challenge calling for further research. As well due to the presence of nanocrystalline particles, which make this fraction of the sample probably the most dangerous for human health.

Supplementary Information The online version contains supplementary material available at https://doi.org/10.1007/s11696-023-03007-8.

Acknowledgements CzechNanoLab Project LM2018110 funded by MEYS CR is gratefully acknowledged for the financial support of the measurements at CEITEC Nano Research Infrastructure.

Funding Open access publishing supported by the National Technical Library in Prague.

Declarations

Conflict of interest On behalf of all authors, the corresponding author states that there is no conflict of interest.

References

Adamiec E (2017) Chemical fractionation and mobility of traffic-related elements in road environments. Environ Geochem Health 39(6):1457–1468. https://doi.org/10.1007/s10653-017-9983-9

Boogaard H, Kos GPA, Weijers EP, Janssen NAH, Fischer PH, van der Zee SC, de Hartog JJ, Hoek G (2011) Contrast in air pollution components between major streets and background locations: particulate matter mass, black carbon, elemental composition, nitrogen oxide and ultrafine particle number. Atmos Environ 45:650–658. https://doi.org/10.1016/j.atmosenv.2010.10.033

Bukowiecki, N, Gehrig R, Lienemann P, Hill M, Figi R, Buchmann B, Furger M, Richard A, Mohr C, Weimer S, Prévôt A, Baltensperger U (2009) PM10 emission factors of abrasion particles from road traffic (APART). Swiss Association of Road and Transportation Experts (VSS). https://trimis.ec.europa.eu/sites/default/files/project/documents/20150710_141622_66365_priloha_radek_1052.pdf Accessed 2 Apr 2022

Chan D, Stachowiak GW (2004) Review of automotive brake friction materials. Proce Inst Mech Eng Part D J Automob Eng 218(9):953–966. https://doi.org/10.1243/0954407041856773

Gerlofs-Nijland ME, Bokkers BGH, Sachse H, Reijnders JJE et al (2019) Inhalation toxicity profiles of particulate matter: a comparison between brake wear with other sources of emission. Inhal Toxicol 31(3):89–98. https://doi.org/10.1080/08958378.2019.1606365

Gonet T, Maher BA (2019) Airborne, vehicle-derived fe-bearing nanoparticles in the urban environment: a review. Environ Sci Technol 53:9970–9991. https://doi.org/10.1021/acs.est.9b01505

Gonser U (1975) From a strange effect to Mossbauer spectroscopy. In: Gonser U (ed) Mossbauer spectroscopy. Springer, Berlin, pp 1–51

Górka-Kostrubiec B, Werner T, Dytłow S, Szczepaniak-Wnuk I, Jeleńska M, Hanc-Kuczkowska A (2019) Detection of metallic iron in urban dust by using high-temperature measurements supplemented with microscopic observations and *Mössbauer spektra*. J Appl Geophys 166:89–102. https://doi.org/10.1016/j.jappgeo.2019.04.022

Gunawardana C, Goonetilleke A, Egodawatta P, Dawes L, Kokot S (2012) Source characterisation of road dust based on chemical and mineralogical composition. Chemosphere 87:163–170. https://doi.org/10.1016/j.chemosphere.2011.12.012

Hinrichs R, Soares MRF, Lamb RG, Soares MRF, Vasconcellos MAZ (2011) Phase characterization of debris generated in brake pad coefficient of friction tests. Wear 270:515–519. https://doi.org/10.1016/j.wear.2011.01.004

Hoek G, Krishnan RM, Beelen R, Peters A, Ostro B, Brunekreef B, Kaufman JD (2013) Long-term air pollution exposure and cardio-respiratory mortality: a review. Environ Health 12:43. https://doi.org/10.1186/1476-069X-12-43W

Hulskotte JHJ, Roskam GD, Denier van der Gon HAC (2014) Elemental composition of current automotive braking materials and derived air emission factors. Atmos Environ 99:436–445. https://doi.org/10.1016/j.atmosenv.2014.10.007

Kelly FJ, Fussell JC (2020) Global nature of airborne particle toxicity and health effects: a focus on megacities, wildfires, dust storms and residential biomass burning. Toxicol Res 9:331–345. https://doi.org/10.1093/toxres/tfaa044

Ketzel M, Omstedt G, Johansson Ch, Düring I, Pohjola M, Oettl D, Gidhagen L, Wåhlin P, Lohmeyer A, Haakana M, Berkowicz R (2007) Estimation and validation of PM2.5/PM10 exhaust and non-exhaust emission factors for practical street pollution modelling. Atmos Environ 41:9370–9385. https://doi.org/10.1016/j.atmosenv.2007.09.005

Kopcewicz B, Kopcewicz M, Pietruczuk A (2015) The Mossbauer study of atmospheric iron-containing aerosol in the coarse and PM2.5 fractions measured in rural site. Chemosphere 131:9–16. https://doi.org/10.1016/j.chemosphere.2015.02.038

Kukutschová J, Roubiček V, Mašlaň M, Jančík D, Slovák V, Malachová K, Pavličková Z, Filip P (2010) Wear performance and wear debris of semimetallic automotive brake materials. Wear 268:86–93. https://doi.org/10.1016/j.wear.2009.06.039

Lawrence S, Sokhi R, Ravindra K, Mao H, Prain HD, Bull ID (2013) Source apportionment of traffic emissions of particulate matter using tunnel measurements. Atmos Environ 77:548–557. https://doi.org/10.1016/j.atmosenv.2013.03.040

Magiera T, Jablonska M, Strzyszcz Z, Rachwal M (2011) Morphological and mineralogical forms of technogenic magnetic particles in industrial dusts. Atmos Environ 45:4281–4290. https://doi.org/10.1016/j.atmosenv.2011.04.076

Maher BA, Ahmed IAM, Karloukovski V, MacLaren DA, Foulds PG, Allsop D, Mann DMA, Torres-Jardón R, Calderon-Garciduenas L (2016) Magnetite pollution nanoparticles in the human brain. PNAS 113(39):10797–10801. https://doi.org/10.1073/pnas.1605941113

Maher BA, González-Maciel A, Reynoso-Robles R, Torres-Jardón R, Calderón-Garcidueñas L (2020) Iron-rich air pollution nanoparticles: an unrecognised environmental risk factor for myocardial mitochondrial dysfunction and cardiac oxidative stress. Environ Res 188:109816. https://doi.org/10.1016/j.envres.2020.109816

Muxworthy AR, Schmidbauer E, Petersen N (2002) Magnetic properties and Mössbauer spectra of urban atmospheric particulate matter: a case study from Munich, Germany. Geophys J Int 150:558–570. https://doi.org/10.1046/j.1365-246X.2002.01725.x

Oudin A, Forsberg B, Nordin Adolfsson A, Lind N, Modig L, Nordin M, Nordin S, Adolfsson R, Nilsson LG (2016) Traffic-related air pollution and dementia incidence in northern Sweden: a longitudinal study. Environ Health Perspect 124:306–312. https://doi.org/10.1289/ehp.1408322

Oroumiyeh F, Jerrett M, Rosario ID, Lipsitt J, Lipsitt J, Liu J, Paulson SE, Ritz B, Schauer JJ, Shafer MM, Shen J, Weichenthal S, Banerjee S, Zhu Y (2022) Elemental composition of fine and coarse particles across the greater Los Angeles area: spatial variation and contributing sources. Environ Pollut 292:118356–118999. https://doi.org/10.1016/j.envpol.2021.118356

Peters R, Ee N, Peters J, Booth A, Mudway I, Anstey KJ (2019) Air pollution and dementia: a systematic review. J Alzheimer's Dis 70:S145–S163. https://doi.org/10.3233/JAD-180631

Roubicek V, Raclavska H, JuchelkovaFilip DP (2008) Wear and environmental aspects of composite materials for automotive braking industry. Wear 265:167–175. https://doi.org/10.1016/j.wear.2007.09.006

Sanderson P, Delgado-Saborit JM, Harrison RM (2014) A review of chemical and physical characterisation of atmospheric metallic nanoparticles. Atmos Environ 94:353–365. https://doi.org/10.1016/j.atmosenv.2014.05.023

Sanders PG, Xu N, Dalka TM, Maricq MM (2003) Airborne brake wear debris: size distributions, composition, and a comparison of dynamometer and vehicle tests. Environ Sci Technol 37:4060–4069

Szumiata T, Gawroński M, Górka B, Brzózka K, Świetlik R, Trojanowska M, Strzelecka M (2013) Chemical, magnetic and Mössbauer effect analysis of road dust from expressway. Nukleonika 58(1):109–112

Švábenská E, Roupcová P, Podstranská I, Petr M, Filip J, Schneeweiss O (2015a) Analysis of the surface layer of the brake disk. In: METAL 2015a—24th international conference on metallurgy and materials, conference proceedings, 886–891, Code 127656, ISBN 978-808729462-8

Švábenská E, Roupcová P, Schneeweiss O (2015b) Analysis of nanoparticles released from the car brakes. In: NANOCON 2015b—7th international conference on nanomaterials—research and application, conference proceedings, pp 548–552

Valotto G, Rampazzo G, Visin F, Gonella F, Cattaruzza E, Glisenti A, Formenton G, Tieppo P (2015) Environmental and traffic-related parameters affecting road dust composition: a multi-technique approach applied to Venice area (Italy). Atmos Environ 122:596–608. https://doi.org/10.1016/j.atmosenv.2015.10.006

Vasconcellos MAZ, Hinrichs R, da Cunha JBM, Soaresc MRF (2010) Mössbauer spectroscopy characterization of automotive brake disc and polymermatrix composite (PMC) pad surfaces. Wear 268:715–720. https://doi.org/10.1016/j.wear.2009.11.011

Wang XS (2016) Investigation of the pollution in the street dust at Xuzhou, China, using magnetic, micro-morphological and Mössbauer spectra analyses. Environ Earth Sci 75:899. https://doi.org/10.1007/s12665-016-5731-1

Žak T, Jiraskova Y (2006) CONFIT: Mossbauer spectra fitting program. Surf Interface Anal 38:710–714. https://doi.org/10.1002/sia.2285